ISSN 1064-2269, Journal of Communications Technology and Electronics, 2023, Vol. 68, No. 9, pp. 1009–1014. © Pleiades Publishing, Inc., 2023.
Russian Text © The Author(s), 2023, published in Radiotekhnika i Elektronika, 2023, Vol. 68, No. 9, pp. 924–929.

ON THE 70th ANNIVERSARY OF THE INSTITUTE OF RADIOENGINEERING AND ELECTRONICS, RUSSIAN ACADEMY OF SCIENCES

Metal–Semiconductor–Metal–ZnS/GaP Detectors for the UV and Visible Spectrum with Electrically Tunable Spectral Photosensitivity

S. V. Averin[a], *, V. A. Zhitov[a], L. Yu. Zakharov[a], V. M. Kotov[a], and M. P. Temiryazeva[a]

[a] *Kotelnikov Institute of Radioengineering and Electronics, Fryazino Branch, Russian Academy of Sciences, Fryazino, Moscow oblast, 141190 Russia*

**e-mail: sva278@ire216.msk.su*

Received May 4, 2023; revised May 4, 2023; accepted May 25, 2023

Abstract—High-quality ZnS epitaxial layers are grown on GaP semiconductor substrates by the MOCVD method. Photodetectors for the visible and UV parts of the spectrum based on interdigital Schottky metal–semiconductor–metal (MSM) barrier contacts to the ZnS/GaP semiconductor structure have been fabricated and studied. The detectors exhibit low dark currents. The dependence of the characteristics of the spectral response of the detectors on the bias voltage is established. It was found that the long-wavelength response limit of ZnS/GaP MSM detectors can shift from 355 to 450 nm when the bias voltage is changed from 10 to 30 V. At the maximum photosensitivity wavelength of 450 nm, the ampere–watt sensitivity of the detector was 0.3 A/W at a bias voltage of 60 V, and the quantum efficiency is 82%.

DOI: 10.1134/S1064226923090024

INTRODUCTION

Semiconductor photodetectors of the UV and visible part of the spectrum are promising for use in many industrial, scientific, and military applications (space, medicine, biology, environmental studies, missile launch warning systems, fire sensors, etc.) [1]. Until recently, only photodetectors based on semiconductor materials Si and GaAs were used to detect light radiation in this region of the spectrum [2, 3]. The disadvantage of such photodetectors is the significant degradation of the parameters ("aging") when exposed to radiation with a photon energy much higher than the band gap of Si and GaAs [2]. Another disadvantage of devices based on Si and GaAs is that their highest sensitivity is in the longer wavelength IR region and noticeably decreases in the visible light and UV regions [2–4].

Wide-gap semiconductors have several advantages when creating photodetectors based on them, since they allow one to realize low dark currents and high sensitivity. In addition, the strength of chemical bonds in wide-gap semiconductor materials leads to their increased radiation resistance, which ensures the reliability of the receiving device under high-energy photon illumination [2]. For these reasons, the development and creation of photodetectors based on wide-gap semiconductor materials is an urgent task of modern optoelectronics, and GaN, ZnO, ZnSe and their solid solutions are currently widely used as active layers of photodetectors in the UV and visible parts of the spectrum [2, 3]. In [5, 6], detectors with a vertical geometry UV Schottky barrier based on wide-gap ZnSe grown on GaAs substrates were studied. The lattice mismatch of ZnSe and GaAs led to a large number of defects in the ZnS epitaxial layer, which caused high dark currents and reduced the sensitivity and efficiency of such detectors. Another problem of detectors with a Schottky barrier is the creation of sufficiently perfect ohmic contacts to wide-gap semiconductor materials. In [7], the *p–i–n*-photodiodes based on ZnSe and ZnMgBeSe with a current sensitivity of 0.17 A/W have been fabricated and investigated. However, the complexity of the diode structure led to problems in integrating the detector with circuits for amplifying and processing the received signal, and the presence of a *p*-layer led to large recombination losses and a significant decrease in the detector sensitivity, which is especially noticeable in the visible and UV parts of the spectrum. In [8], the results of studies of metal–semiconductor–metal (MSM) detectors based on the ZnSTeSe/ZnSe heterostructure are presented. Here, a rather effective broadband detector response is implemented in the spectral range of 305–900 nm with a photosensitivity maximum at a wavelength of ~800 nm due to the presence of a GaAs substrate.

Recently, the authors of [9] published the results of studies of photodetectors based on polymeric perovskite layers. The response of the detector was obtained with the possibility of adjusting the maximum sensitivity in the range of 680–710 nm by choos-

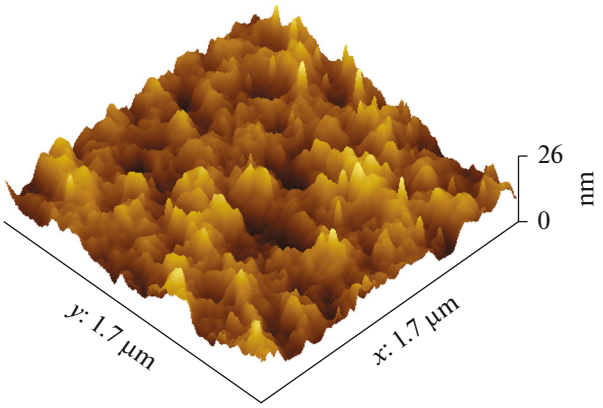

Fig. 1. Micrograph of a fragment of the surface of the ZnS/GaP heterostructure; the thickness of the ZnS epitaxial layer is 255 nm; the root-mean-square irregularity height is 6.3 nm.

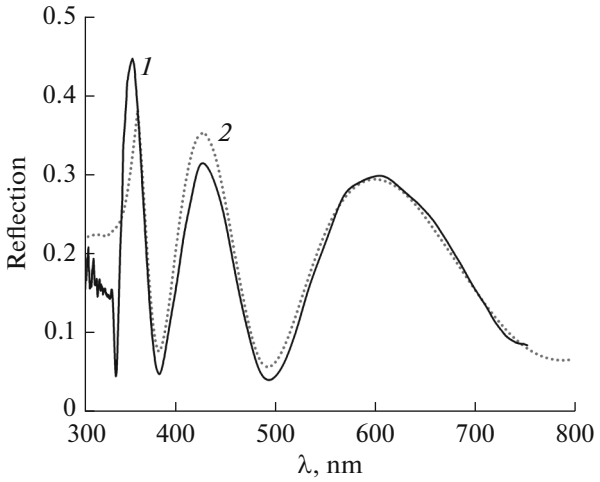

Fig. 2. Experimental (*1*) and calculated (*2*) spectra of the reflection signal from the ZnS/GaP semiconductor structure.

ing polymeric materials with different absorption spectra. Finally, epitaxial GaN MSM detectors with an interdigital contact system have been fabricated and studied quite recently. The detectors are made on sapphire substrates and have a maximum sensitivity to radiation with a wavelength of 350–360 nm [10]. It was found that fast thermal annealing of structures with formed MSM detectors makes it possible to reduce the dark current by a factor of 30. However, even in this case, the dark current was 10 mA at a bias voltage of 2.5 V.

The purpose of this work is to investigate the possibility of controlling the width of the spectral response and the long-wavelength boundary of the UV–visible photodetector by changing the bias voltage. The detector is implemented in the form of interdigitated Schottky MSM barrier contacts to the ZnS/GaP epitaxial structure and provides high ampere–watt sensitivity and low dark current. The long-wavelength response edge of the MSM detector can shift from 355 to 450 nm when the bias voltage changes from 10 to 30 V.

1. RESULTS AND DISCUSSION

An analysis of [5–10] shows that the most promising detector of UV radiation and the visible part of the spectrum is a photodetector based on two rectifying Schottky barrier contacts connected in series in an MSM system [11]. Such a detector allows the use of a semiconductor material of only one type of conductivity, and its planar geometry provides easy integration with amplification and processing circuits for received information signals. Since short-wavelength radiation is absorbed in the high electric field region of the Schottky barrier of the MSM diode, this significantly increases the speed and efficiency of the photodetector and provides a potentially large bandwidth of the optical information system. It should also be noted that for equal capacitance, the area of the active region of the MSM diode is approximately four times larger than the area of the *p–i–n* diode. This noticeably facilitates the focusing of the received optical radiation onto the photosensitive region of the detector [12].

ZnS/GaP semiconductor structures were grown by MOCVD on semi-insulating GaP substrates doped with Cr up to 10^{15} cm^{-3} ($\rho = 10^6$ Ω cm), with a 10-degree deviation of the base plane (100) towards plane (111)A. The structure technology is described in detail in [13]. The surface quality of the grown heterostructure was assessed using a Smart SPM atomic force microscope (AIST-NT).

Figure 1 shows a micrograph of the surface of a ZnS/GaP semiconductor structure with a ZnS epitaxial layer thickness of 255 nm. The root-mean-square height of irregularities on the site of 1.7 × 1.7 μm^2 is 6.3 nm. The thickness of the grown epitaxial layer was calculated from the reflection spectra.

Figure 2 shows the experimental and calculated spectra of the reflection signal from the ZnS/GaP semiconductor structure. The calculated reflection curve is given taking into account interference effects in thin layered structures. To simulate the reflection signal, the matrix method for calculating multilayer structures was used [14]. The refractive index dispersion for GaP was taken from [15], and for ZnS it was obtained from ellipsometry data. The calculated and experimental curves are in good agreement for a ZnS film thickness of 255 nm. The feature in the reflection spectrum at a wavelength of 340 nm corresponds to the ZnS band gap ($E_g = 3.66$ eV).

MSM diodes were fabricated on the grown heterostructures (Fig. 3). Au/Ni films with a total thickness of 210 nm were deposited on the ZnS surface, and interdigital diode contacts were formed by photolithography. According to the measurements, the sur-

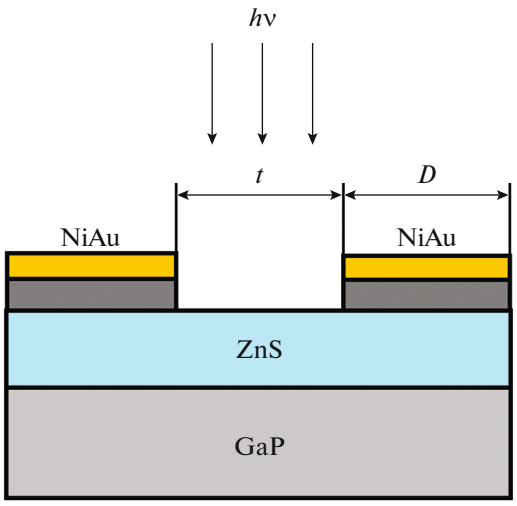

Fig. 3. The structure of the semiconductor layers of the MSM diode and its interdigital contacts.

face roughness of the interdigital contacts of the MSM diodes was 3.4 nm. Two types of MSM detectors were manufactured: D1—with a width of contacts D and gap t between them of 3 μm and D2—with a width of contacts and a gap between them of 10 μm. In this case, the active area of the D1 detector was 100×100 μm^2, and for the D2 detector, 500×500 μm^2.

Simulation within the framework of a one-dimensional model [16] shows that, with such a geometry of the interdigital system of contacts, the response time of detectors D1 and D2 can be 30 and 200 ps, respectively. Figure 4 shows a micrograph of the surface of the ZnS/GaP heterostructure with interdigital Schottky barrier contacts of the D1 MSM diode and the surface profile of the diode structure along conditional line *1*. The width of the contacts and the distance between them is 3 μm.

Measurement of the current–voltage characteristics of the fabricated photodiode structures showed the possibility of operating MSM diodes at high bias voltages with low dark currents (Fig. 5). Detectors allow the use of high operating voltages: samples of D1 photodiode structures, as a rule, withstood a voltage of 80 V without breakdown, and D2, 100 V. Increasing the bias voltage increases the dynamic range of the detector, since it makes it possible to exclude screening effects of the internal field of the diode at high levels of the optical excitation signal of the detector [17]. Measurement of the duration of the photodetector impulse response signal was not carried out due to the lack of a picosecond laser. The dark current of the D1 detector at a bias voltage of 40 V is 2×10^{-11} A, which is an order of magnitude less than the dark current of an MSM diode based on a low-dimensional ZnCdS/ZnMgS/GaP heterostructure [18]. Despite the increased intercontact gap, the dark current of the D2 detector is slightly higher than that of the D1 detector, which is due to the significantly larger active area of the D2 detector [19]. The dark current of the detector largely determines the sensitivity of the photodetector [20, 21]. The low dark currents of the studied diodes confirm the high quality of the grown epitaxial layers.

It is interesting to compare the obtained values of the dark currents of our detectors and the results of other research groups. Thus, an MSM detector based on ohmic contacts to a ZnO film with a photosensitivity maximum at a wavelength of 360 nm had a dark current of 250 nA at a bias of 3 V [22]. The dark current of the MSM detector with Schottky barrier contacts to ZnO with a photosensitivity maximum at a wavelength of 390 nm was 5×10^{-7} A [23]. Finally, the ZnSTeSe MSM photodetector ($t = D = 2$ μm), exhibited a dark current of 5×10^{-10} A at a bias of 40 V [24]. As can be seen, the dark currents realized on MSM diodes D1 and D2 are significantly lower than the dark currents obtained on MSM detectors operating in the same wavelength ranges but made on other semiconductor materials.

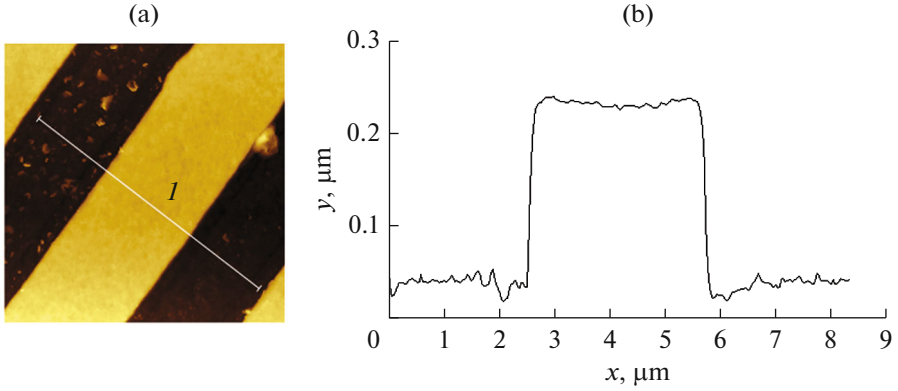

Fig. 4. Micrograph of the surface (a) and the surface profile of the diode MSM structure along conditional line (*1*) (b); the width of the contacts and the distance between them is 3 μm.

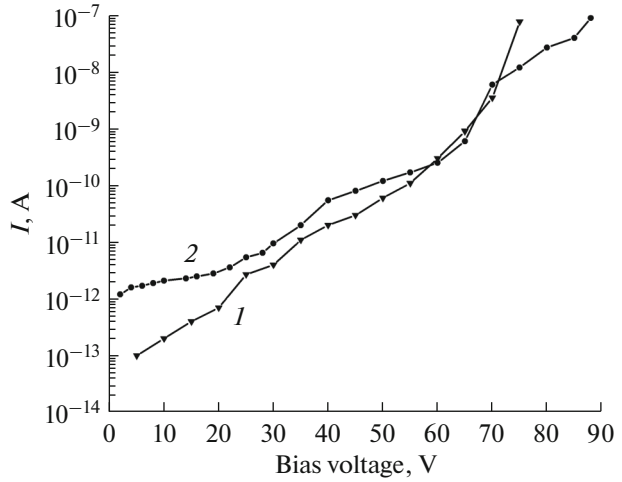

Fig. 5. Dark current of MPM diodes D1 (*1*) and D2 (*2*).

The spectral dependence of the photosensitivity of the MSM detectors was measured using a halogen lamp as a radiation source, a monochromator, a modulator, and a PAR 124 A selective voltmeter using the mode of synchronous detection of the electrical response signal from the MSM photodiode. The ampere–watt sensitivity was determined as the ratio of the detector photocurrent to the power of the optical radiation incident on the MSM diode. The radiation power was measured with a calibrated silicon photodiode.

Figure 6a shows the spectrum of the photoresponse signal of detector D1 at various bias voltages. At small biases, the electric field of the D1 diode with an intercontact gap of 3 μm penetrates only to a small depth, and the detector response is provided by photogeneration and the collection of charge carriers on the contacts of only the upper ZnS layer. The sharp drop in photosensitivity at a bias of 10 V at a wavelength of 340 nm agrees quite well with the band gap of this semiconductor material. The gradual shift of the maximum photosensitivity towards longer wavelengths of optical radiation is explained by the increasing influence of the underlying GaP layer with increasing bias voltage. As a result, at bias voltages exceeding 30 V, there is a significant increase in the detector bandwidth and a shift in its maximum sensitivity by a wavelength of 450 nm, followed by a sharp drop. In this case, the position of the "red" (long-wavelength) response boundary of the studied MSM diode is in good agreement with the threshold energy of direct optical transitions in GaP. In this case, the detector captures the entire violet part of the visible spectrum and its spectral sensitivity is close to the region of the maximum effect of solar pigmentation radiation (360–450 nm) [3]. Thus, the studied photodetector provides effective two-color detection of radiation in the UV and visible parts of the spectrum and at low

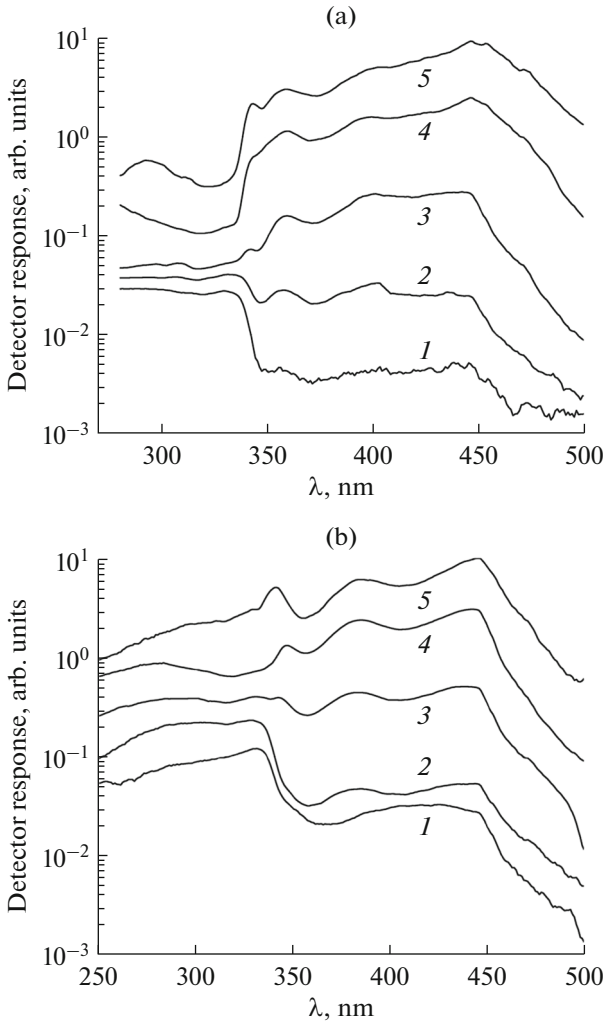

Fig. 6. Dependence of the spectral photosensitivity of MSM detector D1 (a) and D2 (b) on the bias voltage: (a) U_{bias} = 10 (*1*), 20 (*2*), 30 (*3*), 50 (*4*), and 60 V (*5*); (b) U_{bias} = 5 (*1*), 10 (*2*), 15 (*3*), 30 (*4*), and 40 V (*5*).

bias voltages can serve as a detector insensitive to visible light, and at a bias of 40–60 V it can be an effective sunburn sensor. At a bias voltage of 10 V, the ampere–watt sensitivity of detector D1 at a wavelength of 330 nm is 0.1 A/W, and external quantum efficiency (EQE) = 37%. If we take into account that in the MSM detector at $t = D$ at least 50% of the light is reflected from the interdigital contacts, and ~10% from the semiconductor surface in the intercontact region of the MSM diode, then the external quantum efficiency of the D1 detector is close to the theoretically possible one. For comparison, the ampere–watt sensitivity of the AlGaN *p–i–n* photodiode at this wavelength was 0.06 A/W [25]. The current sensitivity of MSM detector D1 at a wavelength of 450 nm at a bias voltage of 60 V was measured to be 0.3 A/W, and EQE = 82%. Taking into account the shading of the active region of the detector by the interdigital con-

tacts of the MSM diode, the internal quantum efficiency of the detector in this case exceeds 100%, and this indicates an internal amplification of the photocurrent in such a diode structure at an increased bias voltage. We believe that the observed photo amplification is due to the capture of minority charge carriers (holes) at the capture centers of the ZnS/GaP heterojunction. The existence of trapping centers at the interface between two semiconductors is well known [26, 27]. It is also known that the capture of charge carriers increases with the applied bias [27]. Hole trapping at the ZnS/GaP heterointerface reduces the effective height of the Schottky barrier when the reverse biased junction of the MSM diode is illuminated, which increases the internal photocurrent amplification of the detector and its quantum efficiency. This is what is observed in our experiment when the bias voltage is increased to 60 V.

The spectral response of the D2 detector (Fig. 6b) essentially does not differ from the response of the D1 detector, but the expansion of the spectral response of the detector in this case occurs at lower bias voltages. This is due to the fact that in structures with a large intercontact gap, the external bias field actively penetrates deep into the MSM diode, and therefore, in our case, even at a bias of 15 V, it is sufficient for efficient collection of charge carriers photogenerated both in the upper ZnS layer of the semiconductor structure of diode D2, and in the GaP layer.

Let us compare the ampere–watt sensitivities obtained by us with the results of other research groups. Schottky barrier photodiodes based on ZnS and ZnSSe demonstrated current sensitivities of 0.08 and 0.09 A/W at wavelengths of 335 and 370 nm, respectively [28]. A $Zn_{0.84}Mg_{0.16}S$ based photodetector at a wavelength of 325 nm had an ampere–watt sensitivity of 0.1 A/W [29]. The current sensitivity of the ZnSe MSM detector of optical radiation at a wavelength of 448 nm was 0.128 A/W, and its quantum efficiency was 36% [30]. Ampere–watt sensitivity of the MSM photodetector based on ZnSTeSe ($t = D = 2$ μm) was equal to 0.4 A/W in the wavelength range of 350–475 nm [24]. Thus, the dark currents and current sensitivities of our detectors are in fairly good agreement with the results obtained by other authors.

CONCLUSIONS

Thus, the following conclusions can be drawn.

MSM detectors of visible and ultraviolet radiation based on the ZnS/GaP heterostructure have been fabricated and studied.

MSM diodes show low dark currents and a strong dependence of the spectral response on the bias voltage. The dark current of ZnS/GaP MSM photodiode structures is 2×10^{-11} A at a bias voltage of 40 V, which is more than an order of magnitude less than that of AlGaN MSM diodes.

By changing the bias voltage, one can change the spectral photosensitivity band of the MSM detector. At low bias voltages, the ZnS/GaP MSM diode is a detector insensitive to visible light. An increase in the bias voltage leads to a significant increase in the broadband of the detector and a shift in its maximum sensitivity by a wavelength of 450 nm, followed by a sharp drop in the photoresponse signal. In this case, the spectral sensitivity of the photodetector captures the area of solar radiation with the maximum pigmentation effect, and the detector can serve as an effective tanning sensor.

ACKNOWLEDGMENTS

We thank P.I. Kuznetsov for providing samples of semiconductor structures.

FUNDING

The study was supported by the state task of the Institute of Kotelnikov Radioengineering and Electronics, Russian Academy of Sciences, project no. 075-01110-23-01.

CONFLICT OF INTEREST

The authors declare that they have no conflicts of interest.

REFERENCES

1. C. Lin, Y. Lu, Y. Tian, et al., Opt. Express **27** (21), 29962 (2019).
2. E. Monroy, F. Omnes, and F. Calle, Semicond. Sci. Technol. **18** (4), R33 (2003).
3. T. V. Blank and Yu. A. Gol'dberg, Semiconductors **37**, 999 (2003).
4. Z. Qin, D. Song, Zh. Xu, et al., Organic Electron. **76**, Article No. 105417 (2020).
5. F. Vigue, E. Tournie, and J.-P. Faurie, Electron. Lett. **36** (4), 352 (2000).
6. E. Monroy, F. Vigue, F. Calle, et al., Appl. Phys. Lett. **77** (17), 2761 (2000).
7. F. Vigue, E. Tournie, and J.-P. Faurie, IEEE J. Quantum Electron. **37** (9), 1146 (2001).
8. W.-R. Chen, T.-H. Meen, and Y. -Ch. Cheng, IEEE Electron Device Lett. **27** (25), 347 (2006).
9. Z. Qin, D. Song, Zh. Xu, et al., Organic Electron. **76**, 105417 (2020).
10. O. A. Sinitskaya, K. Yu. Shubina, D. V. Mokhov, et al., St. Petersburg Polytech. Univ. J.: Phys. Math. **15** (3), 157 (2022).
11. J. B. D. Soole and H. Schumaher, IEEE J. Quantum Electron. **27** (3), 737 (1991).
12. S. V. Averin, Yu. V. Gulyaev, M. D. Dmitriev, et al., Kvantov. Elektron. **23**, 284 (1996).
13. S. V. Averin, P. I. Kuznetsov, V. A. Zhitov, et al., Semiconductors **49**, 1393 (2015).

14. R. M. A. Azzam and N. M. Bashara, *EllipsometrY and Polarized Ligh*t (Amsterdam etc., 1977; Mir, Moscow, 1981).
15. D. E. Aspnes and A. A. Studna, Phys. Rev. B **27** (2), 985 (1983).
16. S. V. Averine, Y. C. Chan, and Y. L. Lam, Solid-State Electron. **45**, 441 (2001).
17. S. V. Averin, P. I. Kuznetzov, and N. V. Alkeev, Tech. Phys. **79**, 1490 (2009).
18. S. V. Averin, P. I. Kuznetzov, V. A. Zhitov, et al., Solid-State Electron. **114**, 135 (2015).
19. S. V. Averin and R. Sachot, Solid-State Electron. **44** (9), 1627 (2000).
20. I.-H. Lee, Phys. Status Solidi A **192** (1), R4 (2002).
21. D.-W. Kim, K.-S. Chea, Y.-J. Park, et al., Phys. Status Solidi A **201**, 2686 (2004).
22. K. W. Liu, J. G. Ma, J. Y. Zhang, et al., Solid-State Electron. **51** (5), 757 (2007).
23. N. N. Janow, F. K. Yam, S. M. Thahab, et al., Current Appl. Phys. **10**, 1452 (2010).
24. S. J. Chang, Y. K. Su, W. R. Chen, et al., IEEE Photonics Technol. Lett. **14** (2), 188 (2002).
25. Z. Yan, S. Jinglan, W. Nili, et al., J. Semiconductors **31**, 124015 (2010).
26. Z. Zhang, H. Wenckstern, M. Schmidt, and M. Grundmann, Appl. Phys. Lett. **99**, 083502 (2011).
27. E. H. Rhoderick and R. H. Williams, *Metal–Semiconductor Contacts* (Oxford. Univ. Press, Oxford, 1988).
28. I. K. So, H. Ma, Z. Q. Zhang, and G. K. L. Wong, Appl. Phys. Lett. **76** (9), 1098 (2000).
29. I. K. Sou, M. C. W. Wu, T. Sun, et al., J. Electron. Mater. **30** (6), 673 (2001).
30. T. K. Lin, S. J. Chang, Y. K. Su, et al., Mater. Sci. Engineering B **119** (2), 202 (2005).